

Flat band magnetism and helical magnetic order in Ni-doped SrCo_2As_2

Yu Li,^{1,2,*} Zhonghao Liu,^{3,†} Zhuang Xu,⁴ Yu Song,¹ Yaobo Huang,⁵ Dawei Shen,³ Ni Ma,³ Ang Li,³ Songxue Chi,⁶ Matthias Frontzek,⁶ Huibo Cao,⁶ Qingzhen Huang,⁷ Weiyi Wang,¹ Yaofeng Xie,¹ Yan Rong,⁴ David P. Young,² J. F. DiTusa,^{2,‡} and Pengcheng Dai^{1,4,§}

¹Department of Physics and Astronomy, Rice University, Houston, TX 77005, USA

²Department of Physics & Astronomy, Louisiana State University, Baton Rouge, LA 70803, USA

³State Key Laboratory of Functional Materials for Informatics and Center for Excellence in Superconducting Electronics, SIMIT, Chinese Academy of Sciences, Shanghai 200050, China

⁴Center for Advanced Quantum Studies and Department of Physics, Beijing Normal University, Beijing 100875, China

⁵Shanghai Synchrotron Radiation Facility, Shanghai Institute of Applied Physics, Chinese Academy of Sciences, Shanghai 201204, China

⁶Quantum Condensed Matter Division, Oak Ridge National Laboratory, Oak Ridge, TN 37831, USA

⁷NIST Center for Neutron Research, National Institute of Standards and Technology, Gaithersburg, MD 20899, USA
(Dated: July 23, 2019)

A series of $\text{Sr}(\text{Co}_{1-x}\text{Ni}_x)_2\text{As}_2$ single crystals was synthesized allowing a comprehensive phase diagram with respect to field, temperature, and chemical substitution to be established. Our neutron diffraction experiments revealed a helimagnetic order with magnetic moments ferromagnetically (FM) aligned in the ab plane and a helimagnetic wavevector of $q = (0, 0, 0.56)$ for $x = 0.1$. The combination of neutron diffraction and angle-resolved photoemission spectroscopy (ARPES) measurements show that the tuning of a flat band with $d_{x^2-y^2}$ orbital character drives the helimagnetism and indicates the possibility of a quantum order-by-disorder mechanism.

The exploration of materials in proximity to quantum phase transitions is a fruitful area for discovering exotic states of matter due to strong quantum fluctuations. This idea can be traced to Villain who coined the name *order-by-disorder* when investigating frustrated insulating magnets [1]. The central idea is that quantum fluctuations, akin to classical entropic effects, can lift the large degeneracy of ground states and favor a particular order, hence the term *order-by-disorder* [2]. This is considered to be the quantum equivalent to the theme used to explain a variety of phenomena including surface tension and DNA folding, and has been employed to explain unconventional superconductivity [3] and even emergent gravity [4]. There is large recent theoretical interest in itinerant ferromagnets in which quantum fluctuations induce a helical state in the vicinity of a quantum critical point [5, 6]. However, experimental evidence for fluctuation-induced helimagnetism is lacking [7]. Meanwhile, as an origin of ferromagnetism complementary to that described by Nagaoka [8], flat-band physics [9] has garnered attention since it provides fertile ground for diverse interaction-driven quantum phases including ferromagnetic (FM) order, Mott insulating phase [10], and superconductivity [11]. Therefore, it is interesting to search for flat-band related helimagnetism in a material close to a FM quantum critical point.

In the AFe_2As_2 ($A = \text{Ca}, \text{Sr}, \text{Ba}$) family of iron pnictides, the superconducting electron pairing is attributed to antiferromagnetic (AF) spin fluctuations [12, 13]. However, FM fluctuations are also suggested [14, 15] and were recently observed in Co-substituted compounds by NMR [16] and neutron scattering experiments [17, 18].

Furthermore, electronic structure calculations [19, 20] and angle resolved photoemission (ARPES) experiments indicate that ACo_2As_2 [17, 21, 22] is in proximity to a FM instability due to the existence of a flat band nearby the Fermi level, although these materials remain paramagnetic down to 2 K with AF low energy spin fluctuations [17]. Since chemical substitution can shift the Fermi level relative to the band structure [23], Ni substitution will drive the system toward Van Hove singularity associated with the flat band and promote the FM instability. Therefore, it is interesting to investigate how AF and FM fluctuations evolve in $\text{A}(\text{Co}_{1-x}\text{Ni}_x)_2\text{As}_2$ and to explore the relevant emergent phenomena.

In this manuscript, we report the results of magnetic susceptibility, χ , and magnetization, M , measurements of $\text{Sr}(\text{Co}_{1-x}\text{Ni}_x)_2\text{As}_2$ with Ni concentrations between 0 and 0.6 [25]. $\text{Sr}(\text{Co}_{1-x}\text{Ni}_x)_2\text{As}_2$ has a ThCr_2Si_2 -type body-centered tetragonal crystal structure and no structural transition above 5 K [Fig. 1(a)] [25]. However, a helical magnetic order was discovered with $q = (0, 0, 0.56)$ and $T_c = 28$ K in $x = 0.1$ [Fig. 1(b-e)]. The critical temperature varies with Ni substitution and has maximum value at $x = 0.1$ [Fig. 2(a,b)]. Our analysis suggests that the ground state is helimagnetic (HM) with moments lying in the ab easy plane while rotating with respect to c -axis in adjacent layers [Fig. 1(b)]. Measurements of $M(H)$ at low temperatures ($2 \text{ K} \leq T \leq 4 \text{ K}$) demonstrate a two-step transition from HM order first into a partially polarized magnetic (PPM) phase and ultimately into a field polarized FM state. Combining neutron diffraction and ARPES experiments, we find a close association between the magnetic moments and a flat band of

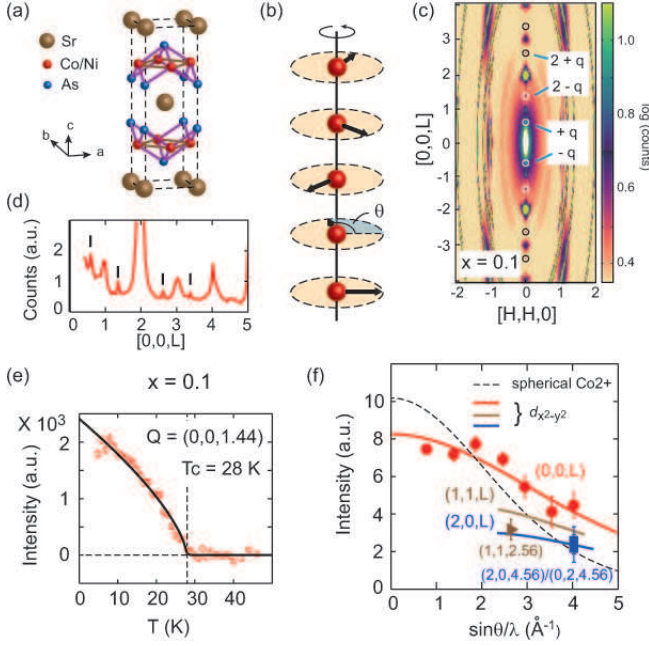


FIG. 1: (a) Tetragonal structure of SrCo₂As₂. (b) Helical magnetic structure along c -axis with a rotation angle θ between neighboring layers. (c) Neutron diffraction measurements on Sr(Co_{0.9}Ni_{0.1})₂As₂ in the $[H,H,L]$ plane [25]. (d) One-dimensional cut along the $[0,0,L]$ direction in (c). (e) Temperature dependence of the magnetic peak at $Q = (0,0,1.44)$ [42]. (f) Integrated intensity of magnetic Bragg peaks. The dashed curve is the magnetic form factor of Co²⁺ using a spherical approximation. The solid curves are magnetic form factors for the $d_{x^2-y^2}$ orbital multiplied with a polarization factor along different measured directions for a helical order. Red, brown and blue are along the $[0,0,L]$, $[1,1,L]$, and $[2,0,L]/[0,2,L]$ directions, respectively.

the $d_{x^2-y^2}$ orbital character. Since BaCo₂As₂ may be a quantum paramagnet near a FM critical point [22, 24], the HM order observed in Sr(Co_{1-x}Ni_x)₂As₂ may be the long-sought fluctuation-induced helimagnetism in the vicinity of the putative quantum critical point [2].

The $\chi(T)$ measured in Sr(Co_{1-x}Ni_x)₂As₂ with $x = 0.125$ is shown in Fig. 2(a). Distinct from nominally pure SrCo₂As₂, where a broad maximum near 100 K [19, 25] is observed, we find a magnetic phase transition for Sr(Co_{0.875}Ni_{0.125})₂As₂ at $T_c = 22$ K, characterized by a maximum in $d(\chi \cdot T)/dT$ [26] for $H = 1$ kOe and H both parallel and perpendicular to the c -axis. For $H = 0.1$ T, $\chi(T < T_c)$ displays a strong dependence on direction of H relative to the crystalline lattice, exhibiting a behavior typical of AF order. In contrast to the A -type AF order in CaCo₂As₂ where spins are ordered along the c -axis, the anisotropy of $\chi(T < T_c)$ for Sr(Co_{1-x}Ni_x)₂As₂ clearly indicates that ab plane is an easy plane [25]. By fitting $\chi(T)$ ($80 \text{ K} < T < 200 \text{ K}$) with the Curie-Weiss law [$\chi(T) \propto (T - T_\theta)^{-1}$], we find a positive T_θ (≈ 28 K for H_{ab} and 25 K for H_c) [25], suggesting that the system is

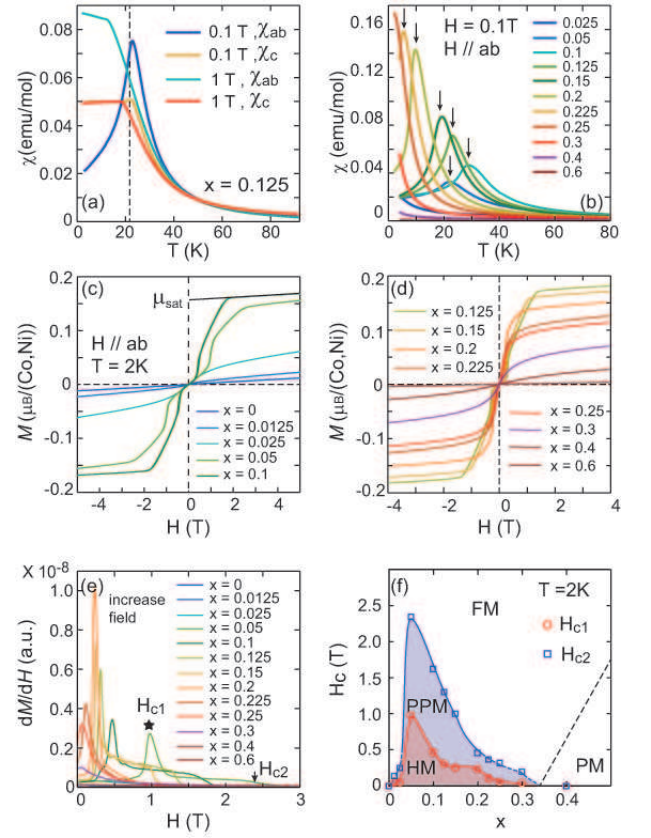


FIG. 2: (a) Magnetic susceptibility, χ , in Sr(Co_{1-x}Ni_x)₂As₂ with field $H = 0.1$ and 1-T parallel and perpendicular to c -axis for $x = 0.125$. (b) $\chi(T)$ for crystals with $0 \leq x \leq 0.6$. (c) and (d) $M(H)$ for these same samples. (e) dM/dH vs. H . (f) Magnetic phase diagram with H and x . H_{c1} and H_{c2} are defined in frame (e). H_{c2} is represented as blue dashed curve where it is poorly determined by the data. The black dashed line is a speculative separation between paramagnetic (PM) and FM states. PPM refers to the partially polarized magnetic state.

dominated by FM interactions. In classical molecular-field theory [27], the parameter $f \equiv T_\theta/T_c$ is usually found to be $-\infty < f < -1$ for antiferromagnets and 1 for ferromagnets, because a transition has to arise before χ diverges at T_θ . However, in our measurements, we found $f > 1$, likely indicating the influence of low dimensionality or disorder. This strongly suggests quantum fluctuations may play significant role [25]. In addition, the large enhancement of $\chi_{ab}(T < T_c)$ with in-plane field at $H = 1$ T suggests the existence of field-induced metamagnetic transition.

In order to understand the evolution of this magnetic state with x , we carried out a systematic exploration of $\chi(T)$ for Sr(Co_{1-x}Ni_x)₂As₂ single crystals. From Fig. 2(b), we see that T_c depends on x in a systematic way creating a dome-like feature in x - T phase diagram with a maximum at $x \sim 0.1$ [Fig. 3(a)]. In Figs. 2(c) and (d), we applied a magnetic field along the ab -plane and

measured $M(H)$ for a series of x . Field-induced transitions associated with the reorientation of magnetic moments were clearly observed in the magnetically ordered compounds. In Fig. 2(c), for example, at $x = 0.1$, as the field increases, a PPM intermediate state arises following a first-order transition [25] at $H_{c1} \sim 0.5$ T and evolves into the field polarized FM state at H_{c2} . These transitions are more clearly observed in dM/dH in Fig. 2(e). We define H_{c1} at the maximum dM/dH . In the intermediate state, dM/dH displays a plateau and H_{c2} was defined as the starting point of the downward step as shown in Fig. 2(e). The plateau in dM/dH shrinks and disappears [Fig. 2(e) and (f)] for $x < 0.05$ or $x \geq 0.2$. Thus, the determination of H_{c2} in these regions is somewhat ambiguous. We display the x - H phase diagram in Fig. 2(f) in which the poorly defined H_{c2} s are represented as dashed lines.

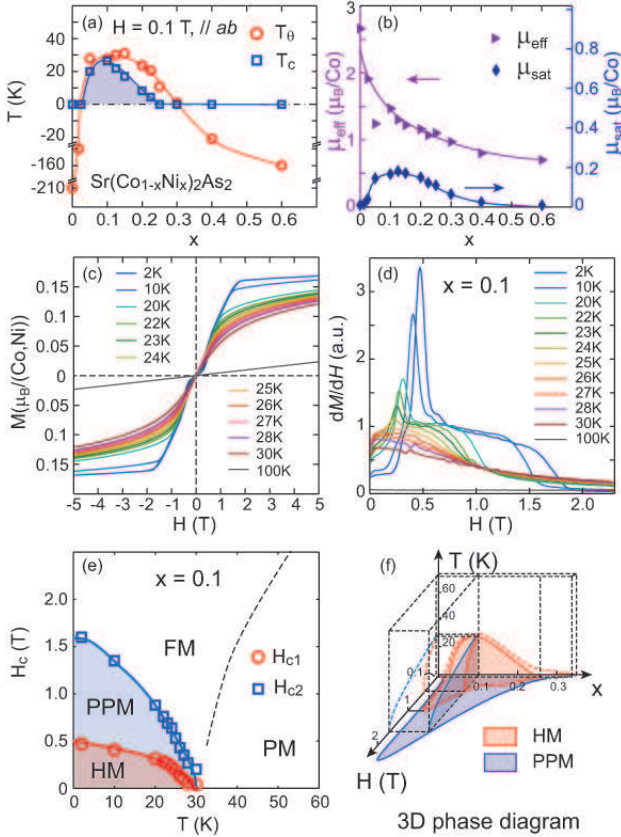


FIG. 3: (a) Critical temperature, T_c , and Weiss temperature T_θ vs. x in $Sr(Co_{1-x}Ni_x)_2As_2$. (b) Effective magnetic moment, μ_{eff} , and saturated magnetic moment, μ_{sat} , vs. x . (c) and (d) M and dM/dH vs. H at temperatures identified in the figures. (e) Phase diagram determined from data in frames (c) and (d). Dashed line is a speculative crossover separating the ferromagnetic, FM, and paramagnetic, PM, phases. PPM denotes the partially polarized magnetic phase. (f) Three dimensional phase diagram combining Figs. 2(f), 3(a) and 3(e).

In Fig. 3(a), we summarize the fitting results of $\chi(T)$

for $0 \leq x \leq 0.6$. Curiously, for Ni concentrations within the dome of magnetic ordering, the dominant interaction, as assessed by T_θ , is ferromagnetic ($T_\theta > 0$) with $f > 1$, while an AF interaction ($T_\theta < 0$) dominates outside this dome. The concurrence of the HM order and the positive T_θ strongly indicates that it is driven by FM interactions. To further explore the changes of the magnetism with x , we plot the effective magnetic moment, μ_{eff} as determined from the Curie constant, and the saturated magnetic moment μ_{sat} , determined from the high field magnetization in Fig. 3(b). The large Rhodes-Wholfarth ratio, μ_{eff} / μ_{sat} , suggests that the magnetism is itinerant in character. Moreover, we have measured $M(H)$ over a range of x and T [Figs. 3(c) and 3(d)]. Based on these data, a H - T phase diagram for $x = 0.1$ is presented in Fig. 3(e) and a schematic three-dimensional (H - T - x) phase diagram is shown in Fig. 3(f).

In order to understand the changes that occur with x in $Sr(Co_{1-x}Ni_x)_2As_2$, we probed the magnetic structure at zero field and $T = 4$ K via neutron diffraction experiments [25]. We chose to explore a $Sr(Co_{0.9}Ni_{0.1})_2As_2$ single crystal as these samples displayed the highest T_c with one of the largest μ_{sat} . Figure 1(c) displays the neutron diffraction pattern in the $[H, H, L]$ scattering plane. Incommensurate peaks at $[0, 0, n \pm q]$ with n an even integer and $q = (0, 0, 0.56)$ are clearly observed. This scattering pattern manifests either a planar spiral or sinusoidal magnetic structure. However, the possibility of sinusoidal order has been excluded by measuring the anisotropy of $\chi(T)$ in the ab plane at low fields [25]. This magnetic structure is substantially different from the collinear AF order in iron pnictides [13] or the commensurate A -type AF order in $CaCo_2As_2$ [28], but is similar to the helical order of magnetic moments associated with the Eu ions in $EuCo_2(P,As)_2$ [29, 30]. In addition, the dissimilar spin anisotropy between $CaCo_2As_2$ [31] and $Sr(Co_{1-x}Ni_x)_2As_2$ [see Fig. 2(a)] suggests a change from easy-axis to easy-plane spin anisotropy. Furthermore, the value of q close to the $(0, 0, 0.5)$ indicates a short pitch of the helix, about 4 Co-layers or 2 unit cells, resulting in spins on adjacent Co-layers being nearly perpendicular. Figure 1(e) shows the T -dependence of the scattering intensity at $Q = (0, 0, 1.44)$. The T_c of 28 K agrees well with $\chi(T)$ [Fig. 2(b)] [25]. In Fig. 1(f), we show the magnetic scattering from neutron diffraction measurements in comparison with the calculated structure factor for helical order. We employed a $d_{x^2-y^2}$ magnetic form factor for Co^{2+} ions [32] and the results (solid lines) are in good agreement with our neutron diffraction measurements. This agreement suggests that the magnetic moments in $Sr(Co_{1-x}Ni_x)_2As_2$ are closely associated with electrons having $d_{x^2-y^2}$ orbital character. The spherical Co^{2+} magnetic form factor (dashed curve) is plotted for comparison and is a much poorer representation of our data.

In nominally pure $SrCo_2As_2$, a flat band exists just

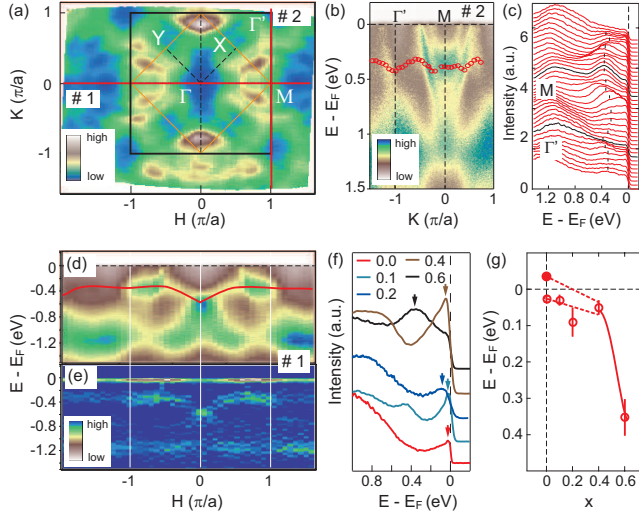


FIG. 4: (a) Plot of the ARPES intensity at E_F of $\text{Sr}(\text{Co}_{0.4}\text{Ni}_{0.6})_2\text{As}_2$. (b),(c) ARPES spectra along the cut #2 direction in frame (a) and its corresponding Energy distribution curve (EDC). (d),(e) Intensity plot and its second-derivative intensity along cut #1 direction. (f) EDC at the M point for $\text{Sr}(\text{Co}_{1-x}\text{Ni}_x)_2\text{As}_2$ for $x = 0, 0.1, 0.2, 0.4$, and 0.6 . (g) The central energy of the flat band for the same materials as in frame (f). Solid circle is the value estimated by DMFT [20]. Dashed lines indicate the uncertainty in the determination of band energies when the EDCs are truncated by the Fermi-Dirac function.

above the Fermi level along $\Gamma - M$ direction [17, 20]. Ni Substitution raises E_F , resulting in a Van Hove singularity associated with this flat band. To establish the connection between the helical order and this flat band, we carried out ARPES experiments on several $\text{Sr}(\text{Co}_{1-x}\text{Ni}_x)_2\text{As}_2$ samples ($x = 0, 0.1, 0.2, 0.4$ and 0.6). Figure 4(a) shows the complex Fermi surfaces of $\text{Sr}(\text{Co}_{1-x}\text{Ni}_x)_2\text{As}_2$ with $x = 0.6$. Two cuts along the horizontal and vertical directions with red lines in Fig. 4(a) both reveal the nearly flat band around -0.4 eV [Figs. 4(b) and 4(d)]. These flat band spectra typically have low intensity [33], but are resolved in the energy distribution curves (EDC) [Fig. 4(c)] and the second-derivative intensity plot [Fig. 4(e)]. To investigate the band shift induced by electron (Ni) doping, we show the EDC cuts at the M point for samples with $0 \leq x \leq 0.6$ in Fig. 4(f). One peak close to E_F associated with the flat band is identified (arrows) and is degenerate with another electron-like band at M [17, 20]. Although the Fermi-Dirac function affects the shape of these peaks, a rough estimate of the band location is sufficient to provide information about the band shift in $\text{Sr}(\text{Co}_{1-x}\text{Ni}_x)_2\text{As}_2$ [Fig. 4(g)]. For SrCo_2As_2 , we plot the estimated energy location from dynamic mean field theory (DMFT) calculation as a solid circle [20]. We find that the band shifting with x at $x < 0.4$ is much slower than that at higher doping ($x > 0.4$). This is a manifestation of the large density

of state (DOS) of the flat band for electrons filling as it shifts across E_F ($0 < x < 0.4$). Since the flat band in SrCo_2As_2 has $d_{x^2-y^2}$ orbital character and makes significant contribution to DOS near E_F [17], our ARPES results for $0 \leq x \leq 0.6$ confirm that this flat band is partially occupied in the range of x with helimagnetism, thus suggesting that the helical magnetic phase is closely associated with this band.

In ACo_2As_2 systems, density function theory (DFT)+DMFT calculations suggest that FM instabilities are due to the flat band near E_F . However, experiments show an evolution from AF order in CaCo_2As_2 [18, 28] to paramagnetism in BaCo_2As_2 (or $\text{Ba}(\text{Fe}_{1/3}\text{Co}_{1/3}\text{Ni}_{1/3})_2\text{As}_2$) with evidence of a nearby FM critical point [22, 24]. This indicates that the magnetism can be tuned by chemical substitution. In SrCo_2As_2 , previous inelastic neutron scattering experiments [17] revealed the coexistence of FM and AF spin fluctuations. It is likely that the fine tuning of these fluctuations by chemical substitution induces the observed magnetic order in $\text{Sr}(\text{Co}_{1-x}\text{Ni}_x)_2\text{As}_2$.

In many helical magnetic systems such as MnSi [35, 36] or $\text{Cr}_{1/3}\text{NbSe}_2$ [37], the helical magnetic order is induced by the Dzyaloshinskii-Moriya (DM) interaction [38] due to the lack of crystalline inversion symmetry. Since $\text{Sr}(\text{Co}_{1-x}\text{Ni}_x)_2\text{As}_2$ has a centrosymmetric crystal structure, the DM interaction is absent. In isostructural EuCo_2P_2 , magnetic moments are associated with Eu ions having $S = 7/2$ [27]. A classical Heisenberg model with a frustrated nearest-neighboring (NN) J_1 and next-nearest-neighboring (NNN) J_2 between basal planes can produce helical order [39, 40]. However, there are difficulties in applying this model to $\text{Sr}(\text{Co}_{1-x}\text{Ni}_x)_2\text{As}_2$. First, the effective spin S derived from $\mu_{eff} = g\sqrt{S(S+1)}$ is only about $1/2$, making the validity of classical Heisenberg model ($S \rightarrow \infty$) questionable. Second, the nearly 90° angle between magnetic moments in adjacent layers determined by $\cos \pi/2 = -J_1/4J_2$ requires an almost vanishing NN exchange coupling J_1 , which appears to be unrealistic. Higher order exchange couplings such as J_3 may help stabilize the helical state but the phase space [41] for a stable helix with a $\sim \pi/2$ rotation angle is limited. Third, although the RKKY interaction which relies on the inter-layer Fe-Fe distance ($\frac{c}{2}$) can contribute to the long-range magnetic interaction in $\text{Sr}(\text{Co}_{1-x}\text{Ni}_x)_2\text{As}_2$ [19], the origin of the helimagnetism is still ambiguous because an unrealistically large k_F ($\sim \frac{\pi}{c}$) is required to make J_1 nearly zero via the spatial oscillation of RKKY interaction.

Alternatively, quantum fluctuations in a paramagnet near a FM instability can make significant contributions to the free energy and stabilize unusual magnetic order [2, 5, 6]. In $\text{Sr}(\text{Co}_{1-x}\text{Ni}_x)_2\text{As}_2$, the massive quantum particle-hole excitations can strongly affect the flat dispersion of $d_{x^2-y^2}$ band along $\Gamma - Z$ direction at the mean-field level and, as a consequence, a helical magnetic or-

der with certain momenta can be induced thereby avoiding a transition to a FM state via the *quantum-order-by-disorder* mechanism.

In conclusion, we discovered a novel helical magnetic order in $\text{Sr}(\text{Co}_{1-x}\text{Ni}_x)_2\text{As}_2$ and established the phase diagram with systematic studies of the magnetic susceptibility. By combining neutron diffraction and ARPES experiments, we have established a close connection between the $d_{x^2-y^2}$ flat band and the helical magnetic order. Based on our results, we claim that the helical magnetic order in $\text{Sr}(\text{Co}_{1-x}\text{Ni}_x)_2\text{As}_2$ is driven by quantum fluctuations and is likely in the vicinity of the quantum critical point.

We thank D.L. Gong, L.Y. Xing, R.Y. Jin, J.D. Zhang, and Ilya Vekhter for helpful discussions. The work at Rice is supported by the U.S. NSF DMR-1700081 and the Robert A. Welch Foundation Grant No. C-1839 (P.D.). This material is based upon the work supported by the U.S. Department of Energy under EPSCoR Grant No. de-sc0012432 with additional support from the Louisiana Board of Regents. The work at ORNL and HFIR was sponsored by the Scientific User Facilities Division, Office of Science, Basic Energy Sciences, U.S. Department of Energy. The ARPES experiment is done in Dreamline, Shanghai Synchrotron Radiation Facility and supported by Ministry of Science and Technology of China (2016YFA0401002) and CAS Pioneer Hundred Talents Program (type C).

* Electronic address: yuli1@lsu.edu

† Electronic address: lzh17@mail.sim.ac.cn

‡ Electronic address: ditusa@phys.lsu.edu

§ Electronic address: pdai@rice.edu

- [1] J. Villain, R. Bidaux, J. P. Carton, R. Conte, J. Phys. **41**, 1263(1980).
- [2] Andrew G. Green, Gareth Conduit, and Frank Krüger, Annu. Rev. Condens. Matter Phys. **9**, 59-77 (2018).
- [3] D. Fay, and J. Appel, Phys. Rev. B **22**, 3173 (1980).
- [4] E. Verlinde, JHEP **04**, 029 (2011).
- [5] G.J. Conduit, A.G. Green, and B.D. Simons. Phys. Rev. Lett. **103**, 207201 (2009).
- [6] M. Uhlarz, C. Pfleiderer, and S.M. Hayden, Phys. Rev. Lett. **93**, 256404 (2004).
- [7] S.J. Thomson, F. Krüger, and A.G. Green, Phys. Rev. B **87**, 224203 (2013).
- [8] Y. Nagaoka, Phy. Rev. **147**, 392 (1966).
- [9] H. Tasaki, Prog. Theor. Phys. **99**, 489 (1998).
- [10] Y. Cao, V. Fatemi, A. Demir, S. Fang, S.L. Tomarken, J.Y. Luo, J.D. Sanchez-Yamagishi, K. Watanabe, T. Taniguchi, E. Kaxiras, R.C. Ashoori, and P. Jarillo-Herrero, Nature **556**, 80 (2018).
- [11] Y. Cao, V. Fatemi, S. Fang, K. Watanabe, T. Taniguchi, E. Kaxiras, and P. Jarillo-herrero, Nature **556**, 43 (2018).
- [12] D. J. Scalapino, Rev. Mod. Phys. **84**, 1383 (2012).
- [13] Pengcheng Dai, Rev. Mod. Phys. **87**, 855 (2015).
- [14] D.J. Singh, and M.-H. Du, Phys. Rev. Lett. **100**, 237003 (2008).
- [15] I.I. Mazin, D.J. Singh, M.D. Johannes, and M.H. Du, Phys. Rev. Lett. **101** 057003 (2008).
- [16] P. Wiecki, B. Roy, D.C. Johnston, S.L. Bud'ko, P.C. Canfield, and Y. Furukawa, Phys. Rev. Lett. **115**, 137001 (2015).
- [17] Yu Li, Zhiping Yin, Zhonghao Liu, Weiyi Wang, Zhuang Xu, Yu Song, Long Tian, Yaobo Huang, Dawei Shen, D.L. Abernathy, J.L. Niedziela, R.A. Ewings, T.G. Perring, D.M. Pajerowski, Masaaki Matsuda, Philippe Bourges, Enderle Mechthild, Yixi Su, Pengcheng Dai, Phys. Rev. Lett. **122**, 117204 (2019).
- [18] A. Sapkota, B.G. Ueland, V.K. Anand, N.S. Sangeetha, D.L. Abernathy, M.B. Stone, J.L. Niedziela, D.C. Johnston, A. Kreyssig, A.I. Goldman, and R.J. McQueeney, Phys. Rev. Lett. **119**, 147201 (2017).
- [19] Abhishek Pandey, D.G. Quirinale, W. Jayasekara, A. Sapkota, M.G. Kim, R.S. Dhaka, Y. Lee, T.W. Heitmann, P. W. Stephens, V. Ogloblichev, A. Kreyssig, R.J. McQueeney, A.I. Goldman, Adam Kaminski, B.N. Harmon, Y. Furukawa, and D.C. Johnston, Phys. Rev. B **88**, 014526 (2013).
- [20] Huican Mao, and Zhiping Yin, Phys. Rev. B **98**, 115128 (2018).
- [21] N. Xu, P. Richard, A. van Roekeghem, P. Zhang, H. Miao, W.-L. Zhang, T. Qian, M. Ferrero, A.S. Sefat, S. Biermann, and H. Ding, Phys. Rev. X **3**, 011006 (2013).
- [22] A.S. Sefat, D.J. Singh, R. Jin, M.A. McGuire, B.C. Sales, and D. Mandrus, Phys. Rev. B **79**, 024512 (2009).
- [23] Z.-H. Liu, A.N. Yaresko, Y. Li, D.V. Evtushinsky, P.-C. Dai, and S.V. Borisenko, Appl. Phys. Lett. **112**, 232602 (2018).
- [24] Yasuyuki Nakajima, Tristin Metz, Christopher Eckberg, Kevin Kirshenbaum, Alex Hughes, Renxiong Wang, Limin Wang, Shanta R. Saha, I-Lin Liu, Nicholas P. Butch, Zhonghao Liu, Sergey V. Borisenko, Peter Y. Zavalij, and Johnpierre Paglione, arXiv:1902.01034v1 (2009).
- [25] See Supplemental Information for more details.
- [26] Michael E. Fisher, Philosophical Magazine **7**(82), 1731-1743 (1962).
- [27] N.S. Sangeetha, Eduardo Cuervo-Reyes, Abhishek Pandey, and D.C. Johnston, Phys. Rev. B **94**, 014422 (2016).
- [28] D.G. Quirinale, V.K. Anand, M.G. Kim, Abhishek Pandey, A. Huq, P.W. Stephens, T.W. Heitmann, A. Kreyssig, R.J. McQueeney, D.C. Johnston, and A.I. Goldman, Phys. Rev. B **88**, 174420 (2013).
- [29] M. Reehuis, W. Jeitschko, M.H. Möller and P.J. Brown, J. Phys. Chem. Solids **53**, 687-690 (1992).
- [30] Xiaoyan Tan, Gilberto Fabbri, Daniel Hasket, Alexander A. Yaroslavl'tsev, Huibo Cao, Corey M. Thompson, Kirill Kovnir, Alexey P. Menushenkov, Roman V. Chernikov, V. Ovidiu Garlea, and Michael Shatruk, J. Am. Chem. Soc. **138**, 2724-2731 (2016).
- [31] W. Zhang, K. Nadeem, H. Xiao, R. Yang, B. Xu, H. Yang, and X.G. Qiu, Phys. Rev. B **92**, 144416 (2015).
- [32] S. Shamoto, M. Sato, J.M. Tranquada, B.J. Sternlieb, and G. Shirane, Phys. Rev. B **48**, 13817 (1993).
- [33] Zhiyong Lin, Jin-Ho Choi, Qiang Zhang, Wei Qin, Seho Yi, Pengdong Wang, Lin Li, Yifan Wang, Hui Zhang, Zhe Sun, Laiming Wei, Shengbai Zhang, Tengfei Guo, Qingyou Lu, Jun-hyung Cho, Changgan Zeng, and Zhenyu Zhang, Phys. Rev. Lett. **121**, 096401 (2018).

- [34] Eleanor M. Clements, Raja Das, Ling Li, Paula J. Lampen-Kelley, Manh-Huong Phan, Veerle Keppen, David Mandrus, and Hariharan Srikanth, *Sci. Rep.* **7**, 6545 (2017).
- [35] C. Dhital, L. DeBeer-Schmitt, Q. Zhang, W. Xie, D.P. Young, and J.F. DiTusa, *Phys. Rev. B* **96**, 214425 (2017).
- [36] S. Mühlbauer, B. Binz, F. Jonietz, C. Pfleiderer, A. Rosch, A. Neubauer, R. Georgii, P. Böni, *Science* **323**, 915-919 (2009).
- [37] N.J. Ghimire, M.A. McGuire, D.S. Parker, B. Sipos, S. Tang, J.-Q. Yan, B.C. Sales, and D. Mandrus, *Phys. Rev. B* **87**, 104403 (2013).
- [38] I. Dzyaloshinskii, *J. Phys. Chem. Solids* **4**, 241 (1958); T.Moriya, *Phys. Rev.* **120**, 91 (1960).
- [39] David C. Johnston, *Phys. Rev. B* **96**, 104405 (2017).
- [40] Takeo Nagamiya, *Phys. Solid State* **20**, 305-411 (1968).
- [41] Takeo Nagamiya, Kazukiyo Nagata, and Yoshiharu Kitano, *Prog. Theor. Phys.* **27**, 1253 (1962).
- [42] The resolution was poor so a small temperature-dependent shift of q (± 0.1) will not affect this measurement.